Quantifying the impact of industrial emissions on clouds

A.C. Povey[1,*], M.W. Christensen[2], G.M. McGarragh[2], C.A. Poulsen[3], S.R. Proud[1], G.E. Thomas[3], R.G. Grainger[1]

[1]*NCEO, Uni. Oxford, UK;* [2]*AOPP, Uni. Oxford, UK;* [3]*RAL Space, UK;* **adam.povey@physics.ox.ac.uk*

Introduction

This poster outlines ongoing work to quantify the variation of cloud effective radius (CER) and cloud albedo (ALB) as a function of aerosol index (AI) by using localised aerosol sources, such as volcanoes, as a natural laboratory. The interaction between aerosols and clouds has been described as the most uncertain aspect of our climate by the IPCC and mapping their relationship will help improve its representation in weather and climate models.

Satellite retrievals by the Optimal Retrieval of Aerosol and Cloud (ORAC) were used, provided by the Climate Change Initiative (CCI) datasets. The data can be downloaded from `http://cci.esa.int`. Further details on the datasets can be found in [1, 2]. ORAC [3, 4] is a generalised optimal estimation scheme [5] to retrieve cloud, aerosol, and surface properties from satellite-based visible and/or infrared measurements. It is open-source software that can be found at `https://github.com/ORAC-CC/orac`.

Localised aerosol sources

The example below shows (a) a false-colour image from AATSR over Hawaii on 9 Sep 2008 and (b) the ORAC retrieval from that image at 1 km resolution, with the wind vector shown by an arrow. A plume of aerosol intermingled with cloud is evident downwind due to passive degassing from Mt. Kilauea.

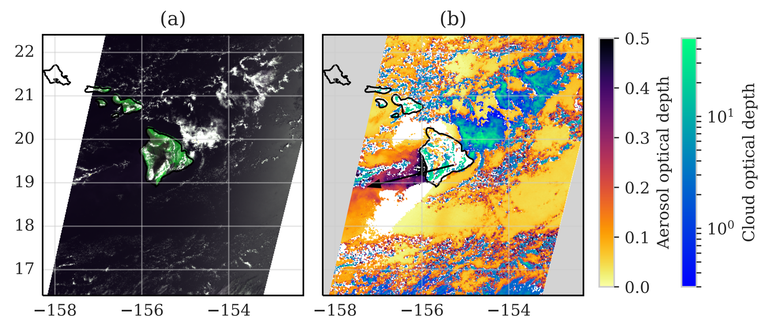

Following [6], when the downwind aerosol is dominated by a single source, one can combine large volumes of data by rotating the image into the direction of the wind, as show above (with the wind blowing from left to right). The result is aerosol and cloud properties as a function of distance and bearing from the source. For a remote site such as this, both clean and polluted conditions will be sampled, mapping cloud properties to the aerosol conditions.

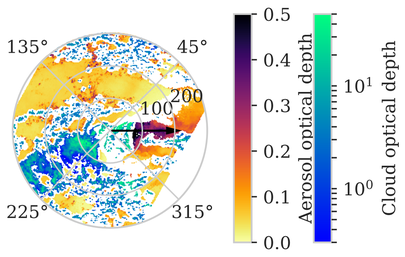

Dominance of the sources

This technique considered 77 natural and anthropogenic aerosol sources and 11 controls, sampling a variety of aerosol types (shown opposite).

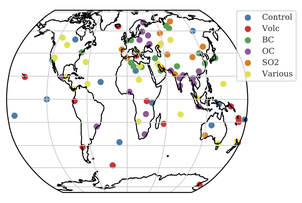

Regularly degassing volcanoes were considered, while frequent flaring identified industrial areas. The CMIP6 inventory highlighted isolated areas of large emissions. The plots below show the difference between aerosol index (AI) downwind and upwind of the sources as a function of (a) absolute distance from the source and (b) days of advection.

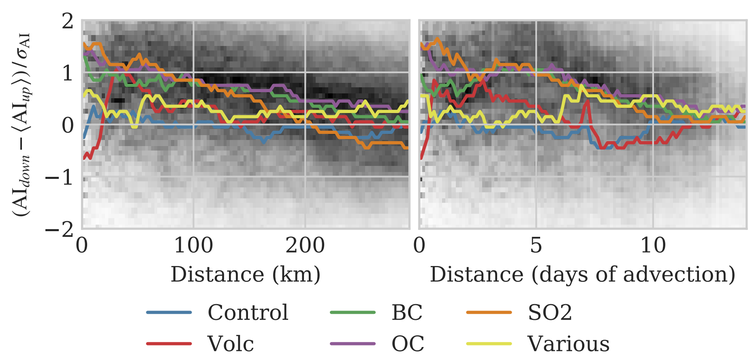

The controls and sites with no dominant aerosol type ('Various') show little change in aerosol enhancement with distance, indicating these sites are not dominant. Other classes affect the AI for about 200 km or 10 days.

Long-term averages

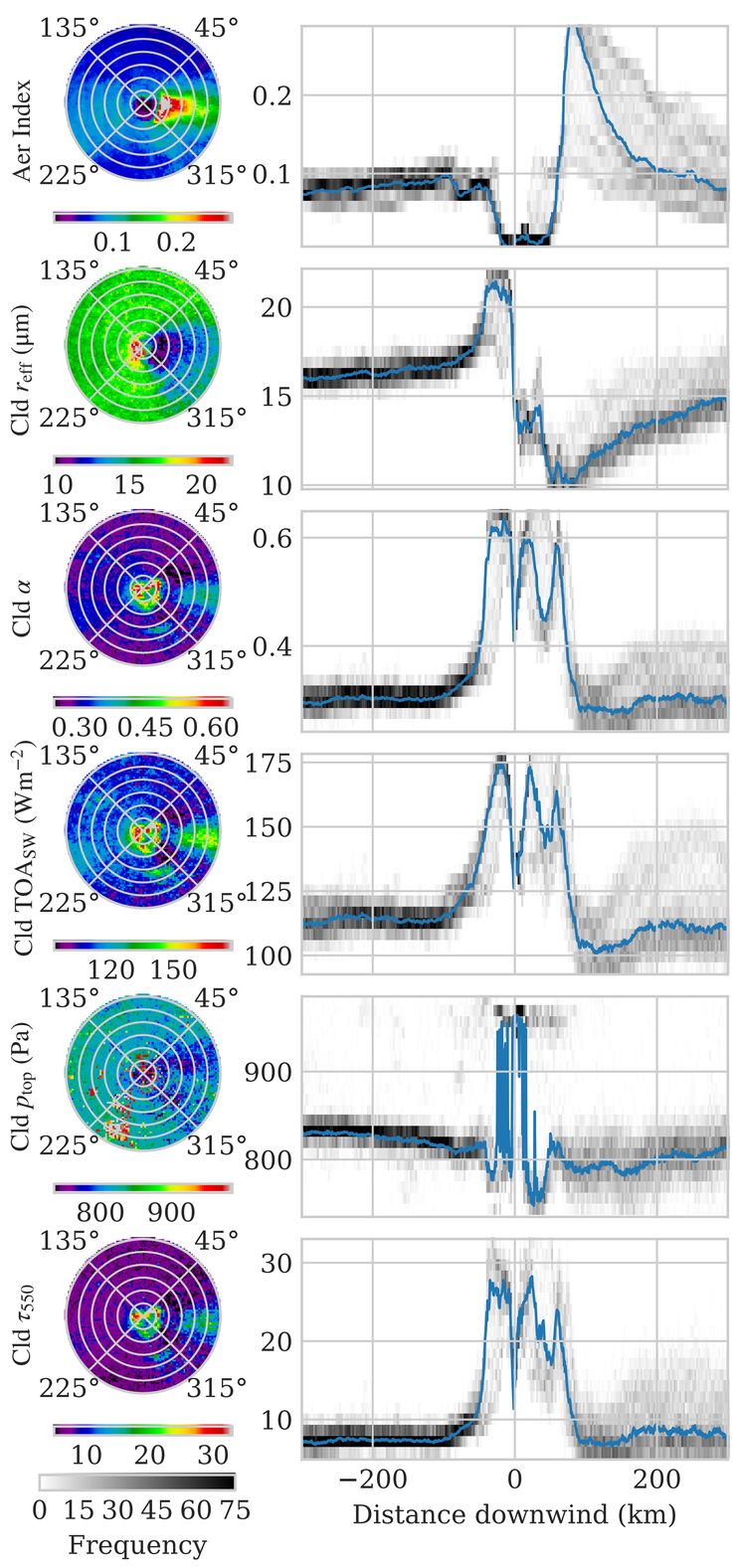

These show distributions around Kilauea for aerosol index, liquid cloud effective radius, cloud albedo, top-of-atmosphere upwelling shortwave radiation, cloud top pressure, and cloud optical depth. The median is shown in blue over the histograms (right). Sharp variations in the centre are caused by the inconsistency of land and sea retrievals and is being alleviated.

Anthropogenic indirect effects

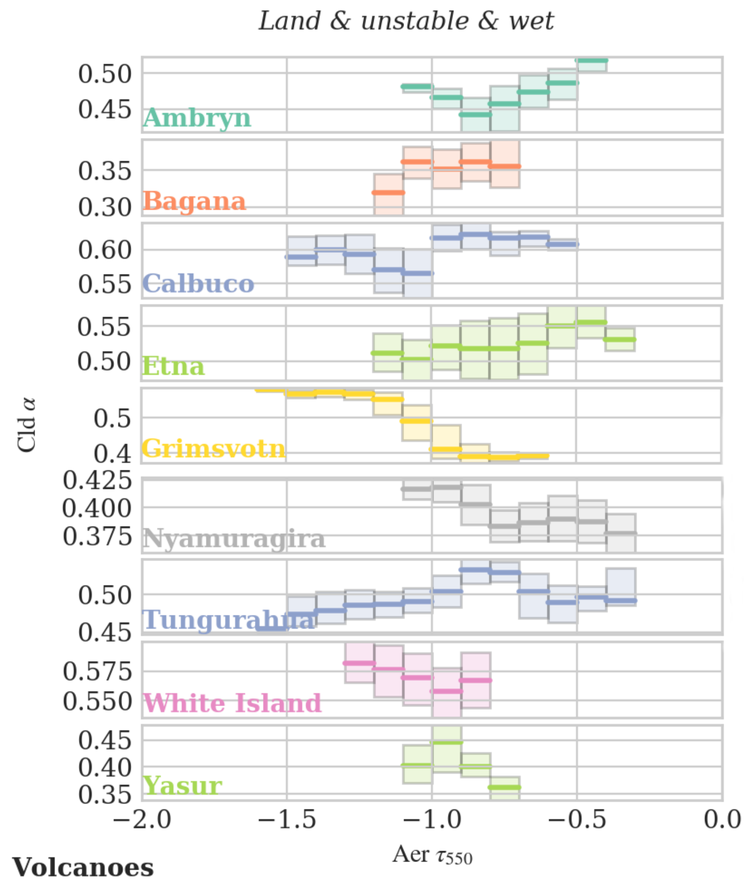

Volcanoes

The cloud-aerosol interactions at various volcanoes are represented with these two-dimensional histograms of cloud albedo against log AI, where each pixel in the rotated field was treated as an independent datum. The expectation that albedo increases with AI is not always observed.

Variation for different aerosol types

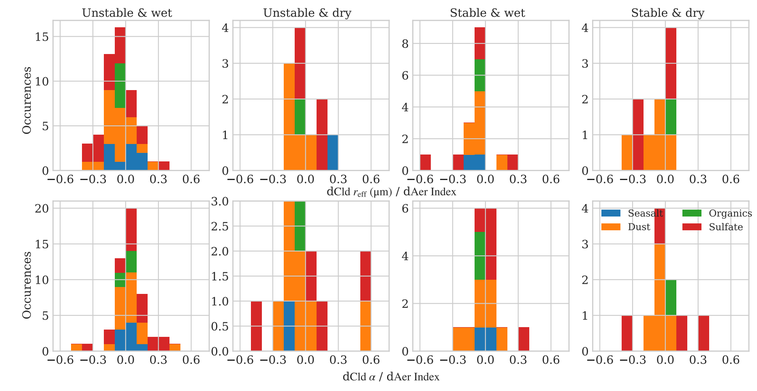

Distribution of the rate of change in CER (top) and ALB (bottom) with AI, divided by meteorological conditions (columns) and the dominant emitted aerosol type (colour). Dust aerosols tend to have negative gradients while sulphates tend to have positive.

A critical look at variation of cloud with aerosol index at Kilauea

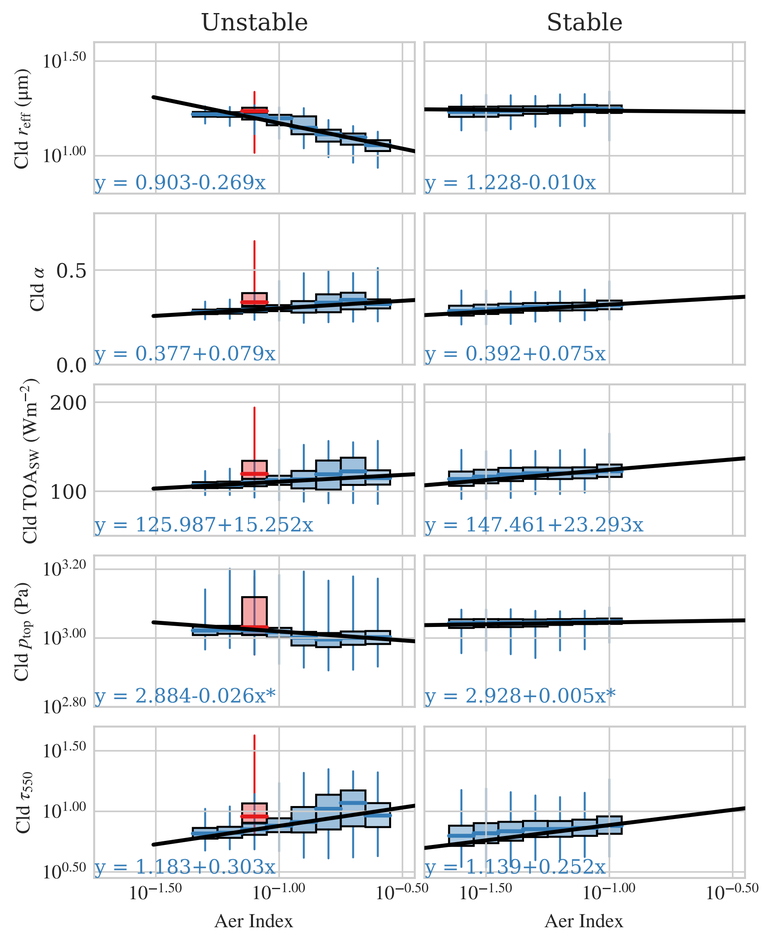

Larger AIs are observed in unstable conditions than stable, which may result from increased AOD in the presence of convection. Cloud effective radius and cloud top pressure decrease with increasing AI in unstable conditions but appear to remain constant in stable conditions. This may be because the effects are only detectable at larger values of AI. Cloud albedo and COD increase at similar rates in both stable and unstable conditions, which implies the change in albedo is dominated by the change in optical thickness or LWP.

Those are confounding variables in this analysis, illustrated in the poster's first figure by the enhanced AOD around cloud. Retrievals within 7 km of a cloud were excluded and, to control for meteorology, pixels were classified as wet/dry and un/stable based on the free tropospheric humidity and lower tropospheric stability reported by ERA-Interim. This was insufficient, considering the results. The analysis will be repeated with more classes of humidity/stability. Also, distances will be normalised by wind speed. A higher resolution land-sea mask will be used to remove the variations seen at the top of this poster and an updated version of the retrieval algorithm utilised.

References

[1] T. Popp et. al. (2016), doi:10.3390/rs8050421.
[2] M. Stengel et. al. (2017), doi:0.5194/essd-2017-48.
[3] G.E. Thomas et. al. (2009), doi:10.5194/amt-2-679-2009.
[4] G.R. McGarragh et. al. (2018), doi:10.5194/amt-11-3397-2018.
[5] C. Rodgers (2000), Inverse Methods for Atmospheric Sounding: Theory and Practice, World Scientific.
[6] S. Ebmeier et. al. (2014), doi:10.5194/acp-14-10601-2014.